

Time-reversal invariant topological superconductivity in doped Weyl semimetals

Pavan Hosur¹, Xi Dai², Zhong Fang² and Xiao-Liang Qi¹

¹*Department of Physics, Stanford University*

²*Institute of Physics, Chinese Academy of Sciences*

Time-reversal invariant topological superconductors are a new state of matter which have a bulk superconducting gap and robust Majorana fermion surface states. These have not yet been realized in solid state systems. In this paper, we propose that this state can be realized in doped Weyl semimetals or Weyl metals. The Fermi surfaces of a Weyl metal carry Chern numbers, which is a required ingredient for such a topological superconductor. By applying the fluctuation-exchange approach to a generic model of time-reversal invariant Dirac and Weyl semimetals, we investigate what microscopic interactions can supply the other ingredient, viz., sign changing of the superconducting gap function between Fermi surfaces with opposite Chern numbers. We find that if the normal state is inversion symmetric, onsite repulsive and exchange interactions induce various nodal phases as well as a small region of topological superconductivity on the phase diagram. Unlike the He³B topological superconductor, the phase here does not rely on any special momentum dependence of the pairing amplitude. Breaking inversion symmetry precludes some of the nodal phases and the topological superconductor becomes much more prominent, especially at large ferromagnetic interaction. Our approach can be extended to generic Dirac or Weyl metals.

I. INTRODUCTION

Nearly a decade after topological insulators took the condensed matter community by storm, interest in topological band structures is bifurcating into two main directions. The first is towards topological superconductors (TSCs)^{1–5}, which are close cousins of topological insulators from a theoretical point of view but are a novel phase nonetheless. They share several properties with the insulators such as a gapped bulk with non-trivial winding of the wavefunction of the occupied bands intimately tied to robust, gapless surface states. However, the surface states in the TSCs are composed of Majorana fermions, in contrast to ordinary electrons in the insulating counterparts. A well-known example of a three-dimensional (3D) TSC is the B-phase of He³, in which fermionic He³ atoms condense into a superconducting state whose gap function has a non-trivial texture in momentum space, thus rendering the superconductor topological⁶. However, there is no known example of a 3D TSC in solid state systems.

The second direction in which interest in topological band structures is heading is towards gapless systems, ushered forth by the discovery of a new 3D phase of matter, dubbed *Weyl semimetals* (WSMs). In this phase, the low-energy electrons behave like Weyl fermions – massless, two-component fermions well-known in high-energy physics and described by the Weyl Hamiltonian $H_{\text{Weyl}} \equiv \hbar v \mathbf{k} \cdot \boldsymbol{\sigma}$, where $\sigma_{x,y,z}$ are the three 2×2 Pauli matrices and \mathbf{k} is momentum^{7–12}. WSMs can be thought of as a 3D version of graphene; however, unlike the Dirac nodes in graphene which can be gapped out by breaking point group symmetries of the honeycomb lattice, Weyl nodes are stable and can only be annihilated via inter-node scattering or via superconductivity. Thus, translational symmetry and charge conservation together render each Weyl node stable against all symmetry preserv-

ing perturbations. This topological feature of their band structure endows WSMs with a host of exotic physical properties, ranging from surface states that form Fermi arcs rather than Fermi surfaces (FSs)^{13,14}, to unusual transport properties hinged on a 3D axial anomaly proportional to the electromagnetic field $\mathbf{E} \cdot \mathbf{B}$ ^{12,15–24}.

Simply put, a WSM emerges when a pair of non-degenerate bands intersects at arbitrary points in momentum space, known as the Weyl nodes. Each Weyl node can be assigned a handedness – right or left – or a *chirality* quantum number $\chi = \pm 1$; the fermion doubling theorem forces Weyl nodes to always come in pairs with opposite chirality^{25,26}. Furthermore, even-ness of chirality under time-reversal (\mathcal{T}) ensures that Weyl nodes in a \mathcal{T} -invariant WSM occur in multiples of four. Since the bands must be non-degenerate, inversion (\mathcal{I}) symmetry is necessarily broken in such a WSM in order to respect Kramer's theorem. A general WSM breaks both \mathcal{T} and \mathcal{I} symmetries and Weyl points may be at different energies, thus turning the system into a Weyl metal phase with a non-vanishing FS.

In this work, we show that \mathcal{T} -invariant Weyl metals are natural hosts for realizing a \mathcal{T} -invariant TSC, and determine the microscopic interactions that cause them to do so. That Weyl metals are convenient starting points for obtaining a TSC can be seen as follows. In a Weyl metal, the FSs carry non-zero Chern numbers of the Berry's phase gauge field. The Chern number on the FS encompassing the j^{th} node, given by

$$C_j = \frac{1}{2\pi} \oint_{\text{FS}_j} d^2 \mathbf{k} \hat{\mathbf{n}}_j(\mathbf{k}) \cdot \nabla_{\mathbf{k}} \times \mathbf{a}_j(\mathbf{k}) \quad (1)$$

where $\mathbf{a}_j(\mathbf{k}) = -i \langle \mathbf{k}, j | \nabla_{\mathbf{k}} | \mathbf{k}, j \rangle$ is the Berry connection for the state $|\mathbf{k}, j\rangle$ on the j^{th} FS and $\hat{\mathbf{n}}_j(\mathbf{k}) = \mathbf{v}_j^F(\mathbf{k}) / |\mathbf{v}_j^F(\mathbf{k})|$ is the FS normal, equals the chirality of the node: $C_j = \chi_j = \pm 1$ irrespective of the sign of the doping. In Ref 27, a simple formula was discovered relating the FS Chern number to topological superconduct-

tivity: given a \mathcal{T} -invariant metal with a set of FSs with Chern numbers $\{C_j\}$, it was shown that the topological invariant ν for a \mathcal{T} -invariant TSC is

$$\nu = \frac{1}{2} \sum_{j \in \text{FS}} C_j \text{sgn}(\Delta_j) \quad (2)$$

where Δ_j is the pairing gap function on the j^{th} FS and is assumed to be much smaller than the Fermi energy in magnitude. \mathcal{T} -symmetry ensures that Δ_j is real, and $\text{sgn}(\Delta_j)$ is well-defined because of the requirement of a fully gapped state. A TSC is implied by $\nu \neq 0$; thus, doped WSMs are natural parent compounds for realizing such a phase since the nontrivial Chern number is already provided by the band structure. The superconducting order parameter need not have a specific momentum-dependence like in He^3B . Instead, it can be momentum-independent on each FS but must alternate in sign between different FSs in any pattern that makes the weighted sum (2) non-vanishing. The question that now begs to be answered is: what microscopic interactions will induce appropriate sign changes in the pairing gap so that the upshot is a TSC?

We answer this question by computing the pairing instabilities in a generic model for a \mathcal{T} -invariant WSM using the fluctuation-exchange approach^{28,29}. The pairing instabilities are generically the eigenstates of the effective interaction vertex at the Fermi level, $\chi_{\mathcal{T}}^{ij}(\mathbf{k}, \mathbf{k}')$, which is defined as the amplitude for two-particle scattering from a pair of Kramer's conjugates $|\mathbf{k}, i\rangle \otimes |\hat{\mathcal{T}}(\mathbf{k}, i)\rangle$ to another pair $|\mathbf{k}', j\rangle \otimes |\hat{\mathcal{T}}(\mathbf{k}', j)\rangle$. To first order in the interactions, the vertex is simply the projection of the bare interaction onto the FS states. Within the fluctuation-exchange prescription, it is obtained to higher orders perturbatively by integrating out states away from the Fermi level. Once $\chi_{\mathcal{T}}^{ij}(\mathbf{k}, \mathbf{k}')$ is determined, the dominant pairing instability is given by the most negative eigenvalue $\lambda_{\mathcal{T}}$ of the linearized gap equation ($\hbar = 1$ henceforth)

$$\sum_j \int_{\mathbf{k}'} \delta(v_j k' - |\mu_j|) \chi_{\mathcal{T}}^{ij}(\mathbf{k}, \mathbf{k}') \Delta_j(\mathbf{k}') = \lambda_{\mathcal{T}} \Delta_i(\mathbf{k}) \quad (3)$$

where μ_j is the chemical potential relative to the j^{th} Weyl point and $\int_{\mathbf{k}'} \equiv \int \frac{d^3 \mathbf{k}'}{(2\pi)^3}$, and the gap function $\Delta_j(\mathbf{k})$ is given by the corresponding eigenvector. If all the eigenvalues are non-negative, there is no pairing instability. When there is an instability, the critical temperature for the phase transition is of the form $T_c \sim \Lambda e^{-1/\rho|\lambda_{\mathcal{T}}|}$ where Λ is an energy cutoff and ρ is the density of states at the Fermi level. Eq. (3) is essentially the statement that the broken symmetry phase that ultimately forms is given by the global minimum of the free energy and corresponds to its most negative eigenvalue.

Physically, a pairing instability exists in \mathcal{T} -symmetric systems because *every* state has a degenerate Kramer's partner with which it can form a Cooper pair and fall into a coherent condensate in the presence of attractive

interactions. In the language of renormalization, this means that only attractive interactions between pairs of Kramer's conjugates states are (marginally) relevant, while all other interactions are either irrelevant or have no flow due to severe phase space constraints. We shall label these Cooper pairs 'type-T'. In \mathcal{I} -symmetric systems, a second type – 'type-I' – of Cooper pairs is also possible where the electrons in the pair are related by \mathcal{I} . The corresponding pairing states are given by the eigenstates of an effective interaction matrix $\chi_{\mathcal{I}}^{ij}(\mathbf{k}, \mathbf{k}')$ analogous to the interaction for type-T states:

$$\sum_j \int_{\mathbf{k}'} \delta(v_j k' - |\mu_j|) \chi_{\mathcal{I}}^{ij}(\mathbf{k}, \mathbf{k}') \Delta_j(\mathbf{k}') = \lambda_{\mathcal{I}} \Delta_i(\mathbf{k}) \quad (4)$$

The leading pairing instability in \mathcal{I} -symmetric systems is then given by the combined lowest eigenvalue of $\chi_{\mathcal{I}}$ and $\chi_{\mathcal{T}}$. More generally, superpositions of type-T and type-I Cooper pairs can exist in systems with both \mathcal{T} - and \mathcal{I} -symmetries. However, we will see later that such mixing is forbidden in our system by symmetry.

Applying the above prescription, for concreteness, on the Hamiltonian for a known Dirac semimetal Na_3Bi ³⁰ and restricting to onsite interactions for simplicity, we find that the TSC forms over a large part of the phase diagram, especially when \mathcal{I} symmetry is broken. In particular, this occurs for purely Ising ferromagnetic interactions ($J_z < 0$) and survives moderate values of Hubbard ($U > 0$) and inter-orbital ($V > 0$) repulsion. If \mathcal{I} -symmetry is restored, most of the TSC is overwhelmed by a nodal phase and only a narrow region near the $V = -J_z$ line survives. Along the way, we unearth various other nodal phases with point or line nodes. These results are summarized in Figs. 4 and 5 and in Table I. We emphasize that although we start with a particular model for Dirac semimetals, our results can straightforwardly be extended to other models by simply reinterpreting the orbital content of the Dirac matrices.

Our work complements two recent works on superconducting instabilities of doped WSMs^{31,32}. Both these works consider \mathcal{I} -symmetric WSMs, which necessarily break \mathcal{T} -symmetry, and study superconducting phases within mean field theory. In contrast, we focus on \mathcal{T} -symmetric WSMs and compute the pairing instabilities using an approach that is more unbiased than mean field theory.

II. NECESSARY CONDITIONS FOR THE TSC

Before presenting the detailed calculation on our model system, we develop some general intuition on the microscopic origins of the TSC. Consider a "minimal" \mathcal{T} -symmetric Weyl metal with four isotropic Weyl nodes,

$$\mathcal{H}_j(\mathbf{k}) = (-1)^j \hbar v_{|j|} \mathbf{k} \cdot \mathbf{\Gamma}_j - \mu_{|j|}, \quad j \in \{1, -1, 2, -2\} \quad (5)$$

where $\mathbf{\Gamma}_j$ are 2×2 Pauli matrices in the basis of the local degrees of freedom at the j^{th} Weyl node, and \mathbf{k} is

the momentum measured with respect to the Weyl point wavevector. The corresponding energy eigenvalues are $\mathcal{E}_j^\pm(\mathbf{k}) = \text{sgn}(\mu_{|j|}) (\hbar v_{|j|} k \pm |\mu_{|j|}|)$. $\mathcal{H}_{\pm j}$ are related by \mathcal{T} and have the same FS Chern number $C_j = (-1)^j$. Isotropy of each Weyl node can be assumed without loss of generality as any anisotropy can be removed by locally rescaling momentum relative to the Weyl node.

For isotropic Weyl nodes, the superconducting gap function projected onto the FSs in any \mathcal{T} -symmetric gapped phase must have the form $\Delta_j(\mathbf{k}) = \Delta_{|j|}$, i.e., it must be independent of \mathbf{k} and the same for Kramer's conjugate FSs. \mathcal{T} -symmetry further requires $\Delta_{|j|} \in \mathbb{R}$. For weak pairing, the Bogoliubov-de Gennes Hamiltonian that describes pairing of Kramer's conjugate Weyl nodes can be written as

$$H_j^{BdG} = \Psi_j^\dagger(\mathbf{k}) \begin{pmatrix} \mathcal{E}_j^-(\mathbf{k}) & \Delta_{|j|} \\ \Delta_{|j|} & -\mathcal{E}_j^-(\mathbf{k}) \end{pmatrix} \Psi_j(\mathbf{k}) \quad (6)$$

where $\Psi_j^\dagger(\mathbf{k}) = (\psi_j^\dagger(\mathbf{k}), \psi_{-j}^\dagger(-\mathbf{k}))$ is the usual Nambu spinor corresponding to $\psi_j^\dagger(\mathbf{k})$, the creation operator for a fermion at the Fermi level at momentum \mathbf{k} relative to the j^{th} Weyl node. The form $\Delta_j(\mathbf{k}) = \Delta_{|j|} \in \mathbb{R}$ block diagonalizes χ_{ij} and simplifies (3) to

$$\begin{pmatrix} \bar{\chi}_{11} & \bar{\chi}_{12} \\ \bar{\chi}_{12} & \bar{\chi}_{22} \end{pmatrix} \begin{pmatrix} \Delta_1 \\ \Delta_2 \end{pmatrix} = \lambda_T \begin{pmatrix} \Delta_1 \\ \Delta_2 \end{pmatrix} \quad (7)$$

where $\bar{\chi}_{ij} = \bar{\chi}_{ji} = \bar{\chi}_{ij}^*$ is $\chi_{\mathcal{T}}^{ij}(\mathbf{k}, \mathbf{k}')$ averaged over \mathbf{k} and \mathbf{k}' on FSs i and j , respectively:

$$\bar{\chi}_{ij} = \int_{\mathbf{k}, \mathbf{k}'} \delta(v_{|i|}k - |\mu_i|) \delta(v_{|j|}k' - |\mu_j|) \chi_{\mathcal{T}}^{ij}(\mathbf{k}, \mathbf{k}') \quad (8)$$

as depicted in Fig 1. We have used fermion antisymmetry in conjunction with $\hat{\mathcal{T}}^2 = -1$ in deriving (7). The topological invariant defined in (2) then reduces to

$$\begin{aligned} \nu &= \frac{1}{2} (2\text{sgn}(\Delta_1) - 2\text{sgn}(\Delta_2)) \\ &= \text{sgn}(\Delta_1) - \text{sgn}(\Delta_2) \end{aligned} \quad (9)$$

Therefore the necessary condition for the TSC is that Δ_1 and Δ_2 have opposite signs. For the TSC to be favored over the trivial state, in which Δ_1 and Δ_2 have the same sign, the criteria $\bar{\chi}_{ij}$ must fulfil are

$$\bar{\chi}_{12} > 0 \text{ and } \begin{cases} \bar{\chi}_{11} + \bar{\chi}_{22} < 0 \\ \bar{\chi}_{11}\bar{\chi}_{22} < (\bar{\chi}_{12})^2 \end{cases} \quad \text{or} \quad (10)$$

These requirements are quite non-trivial. Purely attractive effective interactions violate the first condition and instead give a trivial superconductor. On the other hand, purely repulsive ones satisfy (10) only if inter-FS scattering is stronger than intra-FS scattering, which is unnatural. One way to satisfy these conditions is by including Coulomb repulsion as well as attractive interactions, such as those mediated by phonons, and fine-tuning

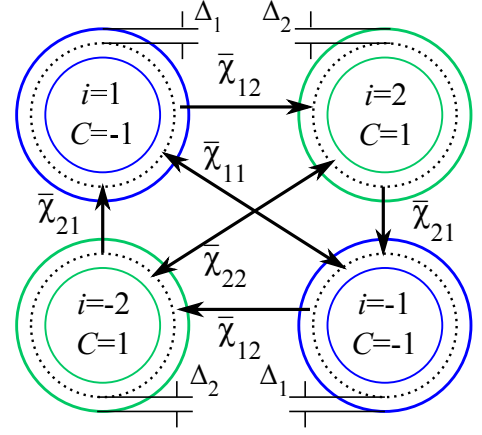


Figure 1: Schematic illustration of the pairing interaction and the gap functions described in Sec II. The dotted circles denote the normal state FSs with index i as discussed in the text and Chern numbers $C = \pm 1$, while the solid lines represent the gaps $\Delta_{1,2}$ in the superconducting state. $\bar{\chi}_{ij}$ is the average Cooper scattering amplitude from Kramer's conjugate states on the $(i, -i)$ FSs to the $(j, -j)$ FSs.

their relative strengths. This way, the net interaction can be made to change sign over large momenta, comparable to the separation of the Weyl nodes, as required by (10). It would, however, be nicer if the necessary momentum dependence emerged naturally without fine-tuning. Note that (10) are not sufficient conditions for a TSC; they ensure that the TSC wins over the trivial superconductor but do not rule out nodal phases.

Eq. (10) are conditions on the effective interactions at the Fermi level. Next, we ask, can an onsite interaction $\mathcal{U}^{\alpha\beta\gamma\delta} \alpha^\dagger \beta^\dagger \gamma \delta$, assumed to be \mathcal{T} -symmetric, give effective interactions that satisfy (10)? Naively, this seems impossible because (10) requires interactions to depend on the FS indices and hence, on momentum, but onsite interactions are momentum-independent³³. However, the effective interaction can acquire momentum dependence in two ways.

Firstly, the FS wavefunctions and hence the operators that project the interactions onto the FSs depend on momentum. That is, projecting \mathcal{U} onto Kramer's conjugate states on the FSs gives χ :

$$\chi_{\mathcal{T}}^{ij}(\mathbf{k}, \mathbf{k}') = \mathcal{U}^{\alpha\beta\gamma\delta} \langle \mathbf{k}', j | \alpha \rangle \langle \hat{\mathcal{T}}(\mathbf{k}', j) | \beta \rangle \langle \gamma | \hat{\mathcal{T}}(\mathbf{k}, i) \rangle \langle \delta | \mathbf{k}, i \rangle \quad (11)$$

which is momentum dependent. However, it turns out that such momentum dependence cannot give a gapped TSC. To see this, we rewrite the \mathbf{k}' -dependent part of the right hand side above as

$$\begin{aligned} \langle \mathbf{k}', j | \alpha \rangle \langle \hat{\mathcal{T}}(\mathbf{k}', j) | \beta \rangle &= -\langle \hat{\mathcal{T}} \beta | \mathbf{k}', j \rangle \langle \mathbf{k}', j | \alpha \rangle \\ &= -\langle \hat{\mathcal{T}} \beta | P_j(\mathbf{k}') | \alpha \rangle, \end{aligned} \quad (12)$$

with $P_j(\mathbf{k}') = |\mathbf{k}', j\rangle \langle \mathbf{k}', j| = \frac{1}{2} \left(1 + \frac{(-1)^j \mathbf{k}' \cdot \mathbf{\Gamma}_j}{k'} \right)$ the

projection operator onto state $|\mathbf{k}', j\rangle$. Clearly, the j -dependent part of $P_j(\mathbf{k}')$ vanishes after integration over \mathbf{k}' . Therefore, $\bar{\chi}_{\mathcal{T}}^{ij}$ obtained by a FS average of $\chi_{\mathcal{T}}^{ij}(\mathbf{k}, \mathbf{k}')$ is independent of the FS indices and cannot support a TSC. In summary, assuming only \mathcal{T} -symmetry and linear dispersion, bare on-site interactions cannot satisfy conditions (10) for a TSC even though the FS effective interaction is momentum dependent.

Secondly, $\chi_{\mathcal{T}}^{ij}(\mathbf{k}, \mathbf{k}')$ receives contributions from virtual processes at higher orders in the bare interactions which are, in general, momentum dependent. A consequence of these induced momentum dependences is that there can be channels in which the gap function Δ is also momentum dependent, in such a way that it sees an effective attractive interaction. In other words, there can be eigenstates $\Delta(\mathbf{k})$ of (3) with negative eigenvalue λ . In the past, such a procedure has been used to predict non-zero angular momentum pairing states induced by Hubbard repulsion^{28,29}. As we will show explicitly in a model system, it is indeed possible to induce a TSC with effective interactions incorporating such second order processes.

As a final note before moving onto the actual calculation for a prototype model, we point out that type-I Cooper pairing in \mathcal{I} -symmetric systems cannot induce topological superconductivity. Since \mathcal{I} relates FSs with opposite Chern numbers, the pair amplitude on each FS necessarily has a phase that winds around some axis passing through the corresponding Weyl node, which in turn requires it to have nodes on the FS. Thus, there are no type-I pairing states that are fully gapped and hence, there is no topological superconductivity.

III. A PROTOTYPE MODEL

Having proven that higher order processes are necessary for obtaining a TSC in a general \mathcal{T} -symmetric WSM, we now apply our analysis to a prototype model which describes a \mathcal{T} -symmetric WSM with minimal number of Weyl points for concreteness. We start from the Dirac semimetal A_3Bi proposed in Ref. 30, with $\text{A}=\text{Na}, \text{K}, \text{Rb}$. Na_3Bi has been recently realized experimentally^{34,35}. Although A_3Bi is a Dirac semimetal³⁶ with two Dirac nodes, it can be thought of as a parent compound for a \mathcal{T} -invariant WSM with four Weyl nodes, because the latter can be obtained from the former via a suitable \mathcal{I} -breaking structural deformation. Below, we first use Na_3Bi as an example to explain the prototype model with \mathcal{I} -symmetry and then discuss the effects of \mathcal{I} -symmetry breaking. Effective interaction terms will be investigated post the description of the band structure. All discussion about the effective model applies to other A_3Bi materials.

A. The prototype model of Dirac semimetal

The crystal structure of Na_3Bi consists of two inequivalent sets of Na atoms, $\text{Na}(1)$ and $\text{Na}(2)$ and one set

of Bi atoms. $\text{Na}(1)$ atoms form a honeycomb lattice with Bi, while $\text{Na}(2)$ are interspersed between the honeycomb layers. The low energy theory near the Dirac point involves four orbitals, including an even parity superposition of the $3s$ orbitals of $\text{Na}(1)$ and $\text{Na}(2)$, henceforth referred to as S , and an odd-parity superposition of the $6 p_x \pm ip_y$ orbitals of Bi atoms in adjacent honeycomb layers, which we shall call P . With spin-orbit coupling, the low energy bands near Fermi level are $|s \uparrow\rangle, |p_x + ip_y, \uparrow\rangle, |s \downarrow\rangle, |p_x - ip_y, \downarrow\rangle$ which have angular momentum quantum number $J_z = \frac{1}{2}, \frac{3}{2}, -\frac{1}{2}, -\frac{3}{2}$ respectively. The low energy effective Hamiltonian of these four bands can be written as $H_0(\mathbf{k}) = c_{\mathbf{k}}^\dagger h_0(\mathbf{k}) c_{\mathbf{k}}$ with

$$\begin{aligned} h_0(\mathbf{k}) &= A(\tau_x \sigma_z k_x - \tau_y k_y) - (M_0 - M_1 k_z^2) \tau_z \\ &\quad + (\epsilon(\mathbf{k}) - \mu) \mathbb{I} \\ &= \begin{pmatrix} M(\mathbf{k}) & Ak_+ & 0 & 0 \\ Ak_- & -M(\mathbf{k}) & 0 & 0 \\ 0 & 0 & M(\mathbf{k}) & -Ak_- \\ 0 & 0 & -Ak_+ & -M(\mathbf{k}) \end{pmatrix} \\ &\quad + (\epsilon(\mathbf{k}) - \mu) \mathbb{I} \end{aligned} \quad (13)$$

Here $c_{\mathbf{k}}$ is a four-component fermion annihilation operator, $\tau_{x,y,z}$ and $\sigma_{x,y,z}$ are Pauli matrices in the orbital and spin-space, respectively, A , M_0 and M_1 are positive constants, $\epsilon_0(\mathbf{k})$ is a \mathbf{k} -dependent energy shift and μ is the chemical potential³⁰. We have denoted $M(\mathbf{k}) = M_0 - M_1 k_z^2$ in the second line above. Note the distinction between $c_{\mathbf{k}}$ and $\psi_j(\mathbf{k})$ introduced in Sec II; the former is a four-component spinor in the spin and orbital basis whereas the latter is a one-component field representing a state at the Fermi level. $h_0(\mathbf{k})$ has Dirac nodes at $\pm K \hat{\mathbf{z}} = \pm \sqrt{M_0/M_1} \hat{\mathbf{z}}$. The symmetries of the system are time reversal $\hat{\mathcal{T}} \equiv i\sigma_y \mathbb{K}$, inversion $\hat{\mathcal{I}} \equiv \tau_z$, spin rotation $\hat{\mathcal{S}}_z \equiv \sigma_z/2$ as well as threefold rotation symmetry about the c -axis. Here \mathbb{K} is the complex conjugation operator. In the long wavelength limit, the threefold rotation symmetry is enlarged to a continuous rotation symmetry $\mathcal{R}_z \equiv -i\partial_\phi - \tau_z \sigma_z/2$ to quadratic order in the momentum, with $-i\partial_\phi$ ($-\tau_z \sigma_z/2$) the orbital (spin) angular momentum.

B. Effects of inversion symmetry breaking

Adding \mathcal{I} breaking terms lifts the degeneracy between the two pairs of Kramers degenerate bands at each Dirac point. For example, a simple term

$$h_1(\mathbf{k}) = 2M_1 \delta K k_z \tau_z \sigma_z \quad (14)$$

splits the two Dirac nodes into four Weyl nodes located at $(\pm K \pm \delta K) \hat{\mathbf{z}}$ to first order in $\delta K/K$, while preserving the symmetries $\hat{\mathcal{R}}_z$, $\hat{\mathcal{S}}_z$ and $\hat{\mathcal{T}}$, as shown in Fig 2.

\mathcal{I} -symmetry breaking has crucial effects on superconductivity. In the \mathcal{I} -symmetric Dirac semimetal, there are two degenerate states at each wavevector on the FS. Thus, a state $|\mathbf{k}, i\rangle$ can generically form a Cooper pair

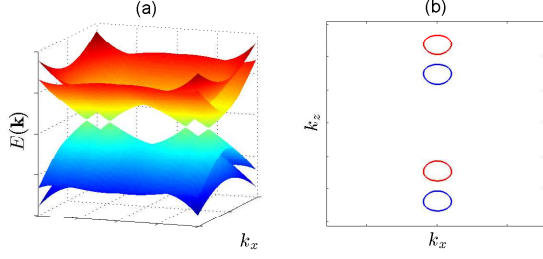


Figure 2: The energy dispersion (a) and the corresponding FS contour (b) in the $k_x - k_z$ plane, for the \mathcal{I} -breaking term given by Eq. (14). The red and blue contours in (b) correspond to spin up and down FSs, respectively.

with a superposition of its time-reversal partner $|\mathcal{T}(\mathbf{k}, i)\rangle$ and inversion partner $|\mathcal{I}(\mathbf{k}, i)\rangle$, i.e., it can form a superposition of a type-T and a type-I Cooper pairs. In the current model, type-T Cooper pairs have total $\mathcal{S}_z = 0$ while type-I Cooper pairs have total $\mathcal{S}_z = \pm 1$. Due to \mathcal{S}_z -conservation, there is thus no mixing between the two types of Cooper pairs. On the other hand, when the two

degenerate bands are split by an \mathcal{I} -breaking term, there is only one state $|\mathbf{k}, i\rangle$ at a generic point at the Fermi level, and the state at opposite momentum is $|\mathcal{T}(\mathbf{k}, i)\rangle$. The inversion partner $|\mathcal{I}(\mathbf{k}, i)\rangle$ now has a different energy and moves away from the Fermi level. As long as the splitting energy scale is much larger than the superconducting gap, Cooper pairing can only occur between the Kramers partners $|\mathbf{k}, i\rangle$ and $|\mathcal{T}(\mathbf{k}, i)\rangle$. In other words, \mathcal{I} -symmetry breaking suppresses some of the pairing channels and thus improves the stability of the \mathcal{T} -invariant superconducting phases, including the TSC that we seek. Indeed, in our fluctuation-exchange calculation that will be discussed later, we find that the TSC phase is much more stable in the absence of \mathcal{I} -symmetry.

C. Effective interaction terms

Next, we discuss interaction terms that are consistent with the symmetries of the system. For A_3Bi , the electron orbitals near the Fermi level are itinerant, so that we can start from the band structure model discussed above, and treat a general short-ranged interaction as a perturbation. To the leading order, it leads to a quartic term in the four-band model:

$$H_{\text{int}} = \sum_{\mathbf{k}, \mathbf{k}', \mathbf{q}, \alpha\beta\gamma\delta} c_{\mathbf{k}+\mathbf{q}, \alpha}^\dagger c_{\mathbf{k}'-\mathbf{q}, \beta}^\dagger c_{\mathbf{k}', \gamma} c_{\mathbf{k}, \delta} g_{\alpha\beta\gamma\delta}(\mathbf{k}, \mathbf{k}', \mathbf{q}) \quad (15)$$

with $g_{\alpha\beta\gamma\delta}(\mathbf{k}, \mathbf{k}', \mathbf{q}) = \int d^3r d^3r' u_{\mathbf{k}+\mathbf{q}, \alpha}^*(\mathbf{r}) u_{\mathbf{k}'-\mathbf{q}, \beta}^*(\mathbf{r}) u_{\mathbf{k}', \gamma}(\mathbf{r}) u_{\mathbf{k}, \delta}(\mathbf{r}) V^{\alpha\beta\gamma\delta}(\mathbf{r} - \mathbf{r}') e^{i\mathbf{q} \cdot (\mathbf{r} - \mathbf{r}')}$

Here $u_{\mathbf{k}\alpha}(\mathbf{r})$ is the periodic part of the Bloch function for the orbital α , with α running over the four orbitals in the effective model, and $V^{\alpha\beta\gamma\delta}(\mathbf{r} - \mathbf{r}')$ is a general short-ranged interaction. Note that there is no sum over the Greek indices in the second line.

We now make the following two simplifying approximations. Firstly, in all materials discussed here, the Weyl points are close to the Γ point in the Brillouin zone, so that we can approximate $u_{\mathbf{k}\alpha}(\mathbf{r})$ by its Γ point value $u_{\mathbf{0}\alpha}(\mathbf{r})$. Secondly, the Fourier transform of short-ranged interaction potential is smooth in \mathbf{q} , so that we can expand the interaction vertex in powers of \mathbf{q} : $g_{\alpha\beta\gamma\delta}(\mathbf{k}, \mathbf{k}', \mathbf{q}) \simeq g_{\alpha\beta\gamma\delta}(\mathbf{0}, \mathbf{0}, \mathbf{q}) \simeq g_{\alpha\beta\gamma\delta}(\mathbf{0}, \mathbf{0}, \mathbf{0}) + \mathbf{q} \cdot \nabla_{\mathbf{q}} g_{\alpha\beta\gamma\delta}(\mathbf{0}, \mathbf{0}, \mathbf{q})|_{\mathbf{q}=\mathbf{0}} + \dots$. To leading order in \mathbf{q} , we approximate the interaction vertex by the momentum independent form $g_{\alpha\beta\gamma\delta}(\mathbf{0}, \mathbf{0}, \mathbf{0}) \equiv g_{0\alpha\beta\gamma\delta}$, which in real space corresponds to approximating the short-range interaction by an on-site interaction. In short, the location of the Weyl nodes close to the Γ -point allows us to strip the interaction of any weak intrinsic momentum dependence. This is justified insofar as the TSC is sought, since a weak momentum dependence cannot change the sign of the interaction over momenta comparable to the splitting

of the Weyl node, which was shown to be necessary condition for the TSC in Sec II.

Either with the approximations above, or phenomenologically, we can now write down the generic form of the on-site interaction vertex $g_{0\alpha\beta\gamma\delta}$ that is consistent with the symmetries of the system, including \mathcal{T} -symmetry, \mathcal{R}_z -symmetry and \mathcal{S}_z -conservation. The allowed terms are:

1. Density-density interactions:

- (a) Hubbard repulsion: $U_S n_{S\uparrow} n_{S\downarrow} + U_P n_{P\uparrow} n_{P\downarrow}$
- (b) Inter-orbital repulsion: $V(n_{S\uparrow} + n_{S\downarrow})(n_{P\uparrow} + n_{P\downarrow})$

2. Ising exchange: $J_z S_i^z \sigma_z^{ij} S_j P_k^\dagger \sigma_z^{kl} P_l$

3. Pair-hopping: $W \left(S_\uparrow^\dagger S_\downarrow^\dagger P_\downarrow P_\uparrow + P_\uparrow^\dagger P_\downarrow^\dagger S_\downarrow S_\uparrow \right)$

Here $S_i = (S_\uparrow, S_\downarrow)$ and $P_i = (P_\uparrow, P_\downarrow)$ are the annihilation operators of the four bands, and $n_S = S_i^\dagger S_i$, $n_P = P_i^\dagger P_i$ are the net fermion numbers in the S and P orbitals, respectively. All these interactions preserve \mathcal{I} symmetry. Moreover, breaking \mathcal{I} symmetry while preserving

the other symmetries does not allow any more terms. If we assume only the three-fold rotation symmetry instead of the continuous rotation symmetry \mathcal{R}_z , more interaction terms will be allowed. However, the effect of these terms to the low energy physics is suppressed since the \mathcal{R}_z -symmetry breaking terms are of order k^3 . Thus, we will only consider the four kinds of interactions listed above.

IV. THE FLUCTUATION-EXCHANGE CALCULATION

We now calculate the effective interaction vertices $\chi_{\mathcal{T}}^{ij}(\mathbf{k}, \mathbf{k}')$ and $\chi_{\mathcal{I}}^{ij}(\mathbf{k}, \mathbf{k}')$ for the prototype model and then use (3) and (4) to find the leading pairing instability. Since we are interested in the physics of the Weyl nodes, we assume $|\mu|, \delta K \ll K$. In this limit, it is reasonable to linearize the Hamiltonian H_0 and work, instead, with

$$H_0(\mathbf{k}) = c_{\mathbf{k}}^\dagger [\tau_x \sigma_z k_x - \tau_y k_y + \nu_z \tau_z k_z - \mu] c_{\mathbf{k}} \quad (16)$$

$$\equiv \sum_j c_{\mathbf{k},j}^\dagger (\Gamma_j \cdot \mathbf{k} - \mu) c_{\mathbf{k},j}$$

where $\Gamma_{j[\sigma,\nu]} \equiv (\langle \sigma_z \rangle \tau_x, -\tau_y, \langle \nu_z \rangle \tau_z)$, i.e., the four Weyl nodes are eigenstates of σ_z and ν_z so that their 2×2 Weyl Hamiltonians can simply be written by replacing σ_z and ν_z in (16) by their eigenvalues. Additionally, momenta have been rescaled to make the nodes isotropic, for convenience, and the Dirac velocity has been set to unity. Note that momentum is now measured from the node. H_0 is the most general Hamiltonian for four degenerate Weyl nodes, because any other suitable Hamiltonian is unitarily related to H_0 and can differ only in the orbital content of the Dirac matrices. Thus, the results obtained here can be straightforwardly extended to other similar systems by appropriate unitary transformations.

Assuming $\mu > 0$ without loss of generality, the wavefunctions for the Fermi level states $|\mathbf{k}, j[\sigma_z, \nu_z]\rangle \equiv |\mathbf{k}, \langle \sigma_z \rangle, \langle \nu_z \rangle\rangle$ are

$$|\mathbf{k}, -, +\rangle \equiv \begin{pmatrix} 1 \\ 0 \end{pmatrix} \otimes \left(-\cos \frac{\theta}{2}, e^{i\phi} \sin \frac{\theta}{2} \right)^T \otimes \begin{pmatrix} 0 \\ 1 \end{pmatrix}$$

$$|\mathbf{k}, +, -\rangle \equiv i\nu_x \sigma_y \mathbb{K} |-\mathbf{k}, -+\rangle$$

$$|\mathbf{k}, -, -\rangle \equiv \nu_x \tau_z |-\mathbf{k}, -+\rangle$$

$$|\mathbf{k}, +, +\rangle \equiv i\nu_x \sigma_y \mathbb{K} |-\mathbf{k}, --\rangle \quad (17)$$

where the first, second and third factors in the direct product refer to the valley (ν), orbital (τ) and spin (σ) parts of the spinors, respectively, and θ and ϕ are the usual spherical polar angles of \mathbf{k} . These spinors will be used to project any interaction onto the FS.

A. First order

To first order in the interactions, the calculation is straightforward and can be done analytically. We simply

project each interaction onto FS states related by \mathcal{T} or \mathcal{I} and obtain the effective interaction matrix $\chi_{\mathcal{O},ij}^X(\mathbf{k}, \mathbf{k}') = \langle \mathbf{k}', j | \langle \mathcal{O}(\mathbf{k}', j) | X | \mathcal{O}(\mathbf{k}, i) \rangle \otimes |\mathbf{k}, i\rangle$ where $i \in \{\pm 1, \pm 2\}$, X is one of the two-body interaction Hamiltonian operators listed in Sec III and $\mathcal{O} = \mathcal{I}, \mathcal{T}$. Once we have the total effective interaction for a particular type of Cooper pairs, $\chi_{\mathcal{O}}(\mathbf{k}, \mathbf{k}') = \sum_X \chi_{\mathcal{O}}^X(\mathbf{k}, \mathbf{k}')$, the pairing instabilities are determined by solving the eigenvalue equations (3) and (4). The results to first order are as follows.

1. Hubbard interaction and pair-hopping:

For simplicity, we first present results for $U_S = U_P = U$. Then, the Hubbard interaction and pair-hopping have the same set of eigenstates for (3) and can be studied together. The effective interaction for non-zero U and W but $V = J_z = 0$ for type-T Cooper pairs is

$$\chi_{\mathcal{T}}^U(\mathbf{k}, \mathbf{k}') + \chi_{\mathcal{T}}^W(\mathbf{k}, \mathbf{k}') = \frac{U+W}{8} \begin{pmatrix} 1 & 1 & 1 & 1 \\ 1 & 1 & 1 & 1 \\ 1 & 1 & 1 & 1 \\ 1 & 1 & 1 & 1 \end{pmatrix}$$

$$+ \frac{U-W}{8} \cos \theta \cos \theta' \begin{pmatrix} 1 & -1 & 1 & -1 \\ -1 & 1 & -1 & 1 \\ 1 & -1 & 1 & -1 \\ -1 & 1 & -1 & 1 \end{pmatrix} \quad (18)$$

This has two sets of eigenstates with non-trivial eigenvalues. They are

$$\Delta_S(\mathbf{k}) = (1, 1, 1, 1)^T, \quad \lambda_0 = \frac{U+W}{2} \quad (19)$$

$$\Delta_{P,n}(\mathbf{k}) = \cos^{2n-1} \theta (1, -1, 1, -1)^T, \quad \lambda_n = \frac{U-W}{4n+2}$$

where $n \in \mathbb{Z} > 0$. All these states preserve \mathcal{T} and \mathcal{I} . Δ_S is gapped while $\Delta_{P,n}$ has a line node at $\theta = \pi/2$. Clearly, a pairing instability exists in one of the above channels when $|W| > U$. If $U_S \neq U_P$, the gap functions develop additional variations over the FSs, but the phase remains the same. Only in the extreme case where one of U_S and U_P vanishes, the gap functions develop additional nodes.

For type-I Cooper pairs, the effective interaction in these channels vanishes. This is because the creation (or annihilation) operators in these interactions are Kramer's conjugates and thus have opposite spins, but type-I Cooper pairs involve equal spin pairing. Thus, projecting the Hubbard or pair-hopping interaction onto states related by \mathcal{I} identically gives zero.

2. Inter-orbital repulsion and Ising exchange:

These two interactions have the same eigenstates for (3) or (4) and can be conveniently studied together. For type-T Cooper pairs, the effective interaction for $U =$

$W = 0$ and non-zero V and J_z is

$$\chi_{\mathcal{T}}^V(\mathbf{k}, \mathbf{k}') + \chi_{\mathcal{T}}^{J_z}(\mathbf{k}, \mathbf{k}') = \frac{V - J_z}{8} \sin \theta \sin \theta' \times \cos(\phi - \phi') \begin{pmatrix} 1 & -1 & -1 & 1 \\ -1 & 1 & 1 & -1 \\ -1 & 1 & 1 & -1 \\ 1 & -1 & -1 & 1 \end{pmatrix} \quad (20)$$

Clearly, only the difference $V - J_z$ is important for type-T Cooper pairs. The eigenstates with non-trivial eigenvalues are

$$\Delta_{\pm}^{\mathcal{T}}(\mathbf{k}) = \sin \theta e^{\pm i\phi} (1, -1, -1, 1)^T, \lambda_{\pm}^{\mathcal{T}} = \frac{V - J_z}{6} \quad (21)$$

These states have point nodes at $\theta = 0, \pi$ and are odd under \mathcal{I} and break \mathcal{T} . A pairing instability exists in this channel if $J_z > V$.

For type-I Cooper pairs, the effective interaction is

$$\chi_{\mathcal{I}}^V + \chi_{\mathcal{I}}^{J_z} = \frac{V + J_z}{4} \sin \theta \sin \theta' \times \begin{pmatrix} e^{i(\phi - \phi')} & 0 & 0 & e^{i(\phi - \phi')} \\ 0 & e^{-i(\phi - \phi')} & e^{-i(\phi - \phi')} & 0 \\ 0 & e^{-i(\phi - \phi')} & e^{-i(\phi - \phi')} & 0 \\ e^{i(\phi - \phi')} & 0 & 0 & e^{i(\phi - \phi')} \end{pmatrix} \quad (22)$$

and has the spectrum

$$\Delta_+^I(\mathbf{k}) = \sin \theta e^{i\phi'} (1 \ 0 \ 0 \ 1)^T, \lambda_+^I = \frac{V + J_z}{3} \quad (23)$$

$$\Delta_-^I(\mathbf{k}) = \sin \theta e^{-i\phi'} (0 \ 1 \ 1 \ 0)^T, \lambda_-^I = \frac{V + J_z}{3} \quad (24)$$

These states are odd under \mathcal{I} , break \mathcal{T} -symmetry and have nodes at $\theta = 0, \pi$. They appear when $J_z < -V$.

Thus, there exist various gapped as well as nodal phases. However, the TSC, given by $\Delta \sim (1, 1, -1, -1)^T$,

is an eigenstate of each interaction with eigenvalue zero. In other words, there is no energy gain in forming the TSC, as we had anticipated in Sec II.

B. Second order

We now consider two-particle scattering processes in the Cooper channel to second order in the bare interactions. The diagrams to this order are depicted in Fig 3. As usual, the solid lines represent fermions and each wavy line denotes any one of the five interactions U_s , U_p , V , J_z and W .

These processes introduce momentum dependence into the interaction. The first two of these processes have been studied in the past for electrons interacting purely via Hubbard repulsion. While the former has been shown to induce spin singlet d -wave superconductivity near a spin density wave instability²⁸, the latter mediates ferromagnetic fluctuations and induces an instability towards

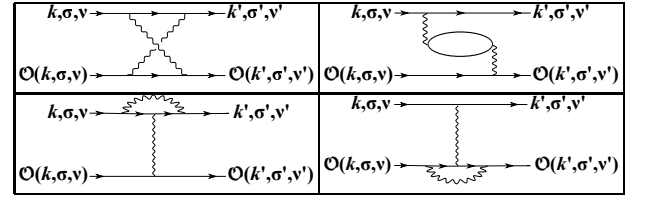


Figure 3: Diagrams that contribute to the effective interaction to second order in the bare interactions. The wavy lines represent any one of the five interactions U_s , U_p , V , J_z and W .

a p -wave superconductor with equal spin pairing²⁹. The bottom row of diagrams does not exist for the Hubbard interactions $U_{s,p}$ or pair-hopping W , but does, for V and J_z . It can be checked that these four diagrams are related to one another by an exchange of a pair of fermion operators for one or both of the bare interactions. Integrating over the internal lines gives

$$\lim_{\beta \rightarrow \infty} \frac{1}{\beta} \sum_{i\omega_n} \int \frac{d\mathbf{k}''}{(2\pi)^3} G_{ab}^{j_1}(i\omega_n, \mathbf{k}'') G_{cd}^{j_2}(i\omega_n, \mathbf{k}'' - \mathbf{Q}) = \begin{cases} -\frac{\Lambda^2}{16\pi^2} \left[\delta_{ab}\delta_{cd} - \frac{1}{3} \mathbf{\Gamma}_{ab}^{j_1} \cdot \mathbf{\Gamma}_{cd}^{j_2} \right] & Q = 0 \\ -\frac{\Lambda^2}{16\pi^2} \left[\delta_{ab}\delta_{cd} + \mathbf{\Gamma}_{ab}^{j_1} \cdot \mathbf{\Gamma}_{cd}^{j_2} - 2(\mathbf{\Gamma}_{ab}^{j_1} \cdot \hat{\mathbf{Q}})(\mathbf{\Gamma}_{cd}^{j_2} \cdot \hat{\mathbf{Q}}) \right] & Q \neq 0 \end{cases} \quad (25)$$

to lowest order in μ/Λ . Here, $G_{ab}^j(i\omega, \mathbf{k}) = [i\omega - \mathbf{\Gamma}_j \cdot \mathbf{k} + \mu]_{ab}^{-1}$ is the Matsubara Green's function of an internal fermion line, $(i\omega_n, \mathbf{k}, j)$ are the internal frequency, momentum relative to the Weyl node and Weyl node index, respectively, Λ is a momentum cut-off which physically corresponds to the scale where non-linearities of the dispersion become important and \mathbf{Q} is the difference in momenta of the internal lines and takes one of

the four values $\pm \mathbf{k} \pm \mathbf{k}'$ depending on the diagram.

The rank-4 tensors in (25) are contracted with the two rank-4 interaction tensors denoted by the wavy lines in Fig 3, the resulting expression is anti-symmetrized with respect to the external lines, and finally projected onto FS states using (17). Although the integrals can be done analytically, the bookkeeping of the diagrams in the presence of all the interactions is best done numerically. Fi-

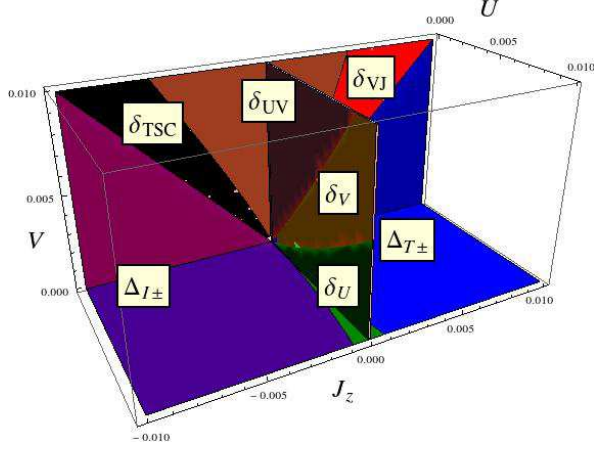


Figure 4: Phase diagram upto second order in the interactions at $W = 0$ in the presence of \mathcal{I} -symmetry. The gray phase at negative J_z and intermediate U or V is the \mathcal{T} -symmetric topological superconductor. The phases were determined numerically, using $\mu = 0.1$ and $\Lambda = 1.0$. Details of all the phases are in Table I.

nally, the first order interactions are added to the results to obtain $\chi_O(\mathbf{k}, \mathbf{k}')$ for each type of Cooper pairs, and the eigenvalue equations (3) and (4) are solved to determine the superconducting phases. The results are discussed in next subsection.

C. Summary of the results

The fluctuation-exchange approach discussed so far can be applied to systems with generic interaction parameters. To understand the result, we make the choice $U_s = U_p \equiv U$ and $W = 0$ and present the phase diagram in the space of J_z, V, U in Figs. 4 and 5. $W = 0$ is chosen on grounds of realizability since it is the least common of all interactions considered here. A small non-zero W clearly does not affect the type-I pairing states to first order because they involve equal spin pairing whereas W involves hopping of Kramers conjugate states which have opposite spin. For type-T pairing states, a straightforward evaluation of the matrix elements of $\chi_{\mathcal{T}}^W$ in the basis of the eigenvectors describing each state shows that δ_U and δ_V are destabilised by W while the other states are unaffected to first order in W .

The black phase labeled δ_{TSC} is the TSC. When \mathcal{I} -symmetry is preserved, δ_{TSC} appears in a narrow range of ferromagnetic J_z and repulsive V , and is dominated by a nodal phase if either of these interactions is enhanced. Importantly, the nodal phase at large ferromagnetic J_z is an equal spin pairing state, consisting of type-I Cooper pairing, and is thus precluded if \mathcal{I} -symmetry is broken. In the absence of \mathcal{I} -symmetry, therefore, δ_{TSC} appears over a much larger region of the phase diagram. In particular, it forms if interactions are purely ferromagnetic,

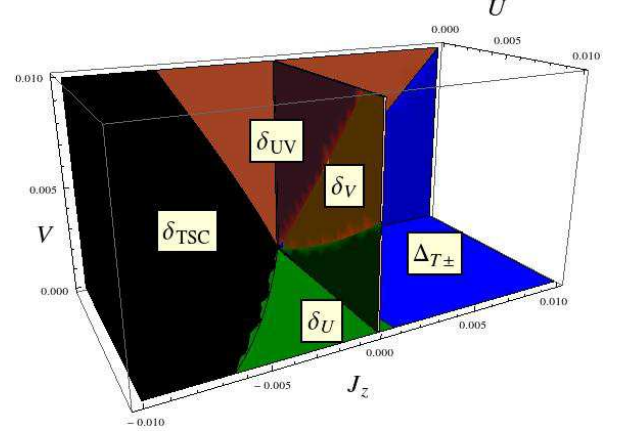


Figure 5: Phase diagram upto second order in the interactions at $W = 0$ in the absence of \mathcal{I} -symmetry. The black phase at negative J_z is the \mathcal{T} -symmetric TSC, which occupies a larger part of the phase diagram compared to Fig 4 when \mathcal{I} -symmetry is present. The phases were determined numerically, using $\mu = 0.1$ and $\Lambda = 1.0$. The $J_z = 0$ cross-section is identical to the one in Fig 4. Details of all the phases are in Table I.

Phase	Cooper pair	\mathcal{T}	Nodal structure	ϕ -dependence
$\Delta_{T\pm}$	T-type	\times	2 point nodes	$e^{\pm i\phi}$
$\Delta_{I\pm}$	I-type	\times	2 point nodes	$e^{\pm i\phi}$
δ_{TSC}	T-type	\checkmark	gapped	none
δ_U	T-type	\checkmark	2 line nodes	none
δ_V	T-type	\times	2 point, 1 line	$e^{\pm i\phi}$
δ_{UV}	T-type	\times	2 point nodes	$e^{\pm 2i\phi}$
δ_{VJ}	I-type	\times	2 point, 2 line	$e^{\pm i\phi}$

Table I: Details of the phases in Figs. 4 and 5. Δ -phases (δ -phases) appear to first (second) order in the interactions. ϕ is the azimuthal angle in momentum space. The phases with no ϕ -dependence are non-degenerate while the rest are doubly degenerate, with one state corresponding to each sign in the ‘ ϕ -dependence’ column. δ_{TSC} is the topological superconductor.

and survives moderate V and U .

We make a quick note about a subtlety of the type-I pairing states. Since the FSs have Chern numbers, the wavefunctions on them cannot be defined globally. For any phase choice of the wavefunction, each FS has a point around which the phase of the wavefunction winds, but the magnitude is non-vanishing. Consequently, the gap functions projected onto the Fermi level are not smooth either even though the Cooper pair wavefunctions written in terms of the underlying orbitals are. This is not an issue for the type-T Cooper pairs, because the phases of wavefunctions of Kramer’s conjugates mutually cancel.

V. CONCLUSION AND DISCUSSIONS

In summary, we have proposed a general procedure for the search of \mathcal{T} -invariant topological superconductivity in doped WSMs. The nontrivial Berry curvature at the FSs of WSMs allows the TSC to be realized for a pairing function with no special momentum dependence like in He^3B . Using the fluctuation-exchange approach, we discovered the general requirements on the effective interaction for the realization of a TSC phase using a minimal model of \mathcal{T} -invariant WSM. As an explicit example, we study a prototype model describing Dirac semimetal A_3Bi and its \mathcal{I} -breaking deformation. We studied explicitly the possible interaction terms up to second order of the bare interaction, and obtained the phase diagram of possible superconductor phases. We showed that the TSC exists when the ferromagnetic exchange coupling is greater than or comparable to the repulsive density-density interactions, and is stabilised greatly by the violation of \mathcal{I} -symmetry. Thus, our results suggest searching for the TSC phase in doped A_3Bi family of materials. Interestingly, another Dirac semimetal, Cd_3As_2 , was theoretically predicted³⁷ and experimentally realized^{38–41} recently. Different from A_3Bi , Cd_3As_2 is proposed to be \mathcal{I} -breaking, although the \mathcal{I} -breaking does not separate the Weyl points, but instead induces a velocity anisotropy³⁷. Nonetheless, it would be extremely interesting to investigate what kinds of superconductivity are possible in this material; in particular, is it a better candidate for possible TSCs than A_3Bi , since it already breaks inversion symmetry?

Although we used the prototype model as an example, our proposal of realizing TSC in doped WSM is generic and can apply to other doped WSM systems with suitable electronic interactions. The general idea is that the topological nontrivial FSs in doped WSM already provide a suitable normal state for TSC, and the inversion symmetry breaking helps to suppress other competing superconducting orders. For a given doped WSM system, the fluctuation-exchange method can be used to determine whether the electron interaction in this system prefers TSC. Now that the list of WSMs and Dirac semimetals is growing rapidly, our proposal provides a guiding principle and a general method for the search of a 3D TSC in this large family of materials. An interesting future direction is to generalize this approach to systems with degenerate points on the FSs, *i.e.*, touching points of multiple FSs. In such cases, the pairing order parameter can generically take a matrix form at the degenerate points, allowing richer possibilities for superconductivity.

ACKNOWLEDGMENTS

PH would like to thank Srinivas Raghu for helpful discussions and David and Lucile Packard Foundation as well as the Department of Energy Office of Basic Energy Sciences, contract DE-AC02-76SF00515 for financial support. XD and ZF acknowledge support from the National Science Foundation of China and the 973 Program of China (No. 2011CBA00108 and No. 2013CB921700). XLQ is supported by the National Science Foundation through the grant No. DMR-1151786.

-
- ¹ A. Kitaev, L. D. Landau Memorial Conference “Advances in Theoretical Physics” (AIP, 2009) pp. 22–30.
 - ² A. Y. Kitaev, *Physics-Uspekhi* **44**, 131 (2001).
 - ³ L. Fu and E. Berg, *Phys. Rev. Lett.* **105**, 097001 (2010).
 - ⁴ X.-L. Qi and S.-C. Zhang, *Rev. Mod. Phys.* **83**, 1057 (2011).
 - ⁵ A. P. Schnyder, P. M. R. Brydon, D. Manske, and C. Timm, *Phys. Rev. B* **82**, 184508 (2010).
 - ⁶ G. Volovik, *The Universe in a Helium Droplet*, International Series of Monographs on Physics (Oxford University Press, 2009).
 - ⁷ X. Wan, A. M. Turner, A. Vishwanath, and S. Y. Savrasov, *Phys. Rev. B* **83**, 205101 (2011).
 - ⁸ O. Vafeek and A. Vishwanath, *ArXiv e-prints* (2013), arXiv:1306.2272 [cond-mat.mes-hall].
 - ⁹ A. M. Turner and A. Vishwanath, *ArXiv e-prints* (2013), arXiv:1301.0330 [cond-mat.str-el].
 - ¹⁰ W. Witczak-Krempa and Y.-B. Kim, *Phys. Rev. B* **85**, 045124 (2012).
 - ¹¹ G. Chen and M. Hermele, *Phys. Rev. B* **86**, 235129 (2012).
 - ¹² P. Hosur and X. Qi, *Topological insulators / Isolants topologiques* *Topological insulators / Isolants topologiques*, *Comptes Rendus Physique* **14**, 857 (2013).
 - ¹³ T. Heikkilä, N. Kopnin, and G. Volovik, *JETP Letters* **94**, 233 (2011).
 - ¹⁴ P. Hosur, *Phys. Rev. B* **86**, 195102 (2012).
 - ¹⁵ V. Aji, *Phys. Rev. B* **85**, 241101 (2012).
 - ¹⁶ H. B. Nielsen and M. Ninomiya, *Physics Letters B* **130**, 389 (1983).
 - ¹⁷ A. A. Zyuzin and A. A. Burkov, *Phys. Rev. B* **86**, 115133 (2012).
 - ¹⁸ D. T. Son and B. Z. Spivak, *Phys. Rev. B* **88**, 104412 (2013).
 - ¹⁹ A. G. Grushin, *Phys. Rev. D* **86**, 045001 (2012).
 - ²⁰ S. A. Parameswaran, T. Grover, D. A. Abanin, D. A. Pesin, and A. Vishwanath, *ArXiv e-prints* (2013), arXiv:1306.1234 [cond-mat.str-el].
 - ²¹ G. Basar, D. E. Kharzeev, and H.-U. Yee, *ArXiv e-prints* (2013), arXiv:1305.6338 [hep-th].
 - ²² K. Landsteiner, *ArXiv e-prints* (2013), arXiv:1306.4932 [hep-th].
 - ²³ C.-X. Liu, P. Ye, and X.-L. Qi, *Phys. Rev. B* **87**, 235306 (2013).
 - ²⁴ Z. Wang and S.-C. Zhang, *Phys. Rev. B* **87**, 161107 (2013).
 - ²⁵ H. Nielsen and M. Ninomiya, *Nuclear Physics B* **185**, 20 (1981).

- ²⁶ H. B. Nielsen and M. Ninomiya, Nuclear Physics B **193**, 173 (1981).
- ²⁷ X.-L. Qi, T. L. Hughes, and S.-C. Zhang, Phys. Rev. B **81**, 134508 (2010).
- ²⁸ D. J. Scalapino, E. Loh, and J. E. Hirsch, Phys. Rev. B **34**, 8190 (1986).
- ²⁹ S. Raghu, S. A. Kivelson, and D. J. Scalapino, Phys. Rev. B **81**, 224505 (2010).
- ³⁰ Z. Wang, Y. Sun, X.-Q. Chen, C. Franchini, G. Xu, H. Weng, X. Dai, and Z. Fang, Phys. Rev. B **85**, 195320 (2012).
- ³¹ G. Y. Cho, J. H. Bardarson, Y.-M. Lu, and J. E. Moore, Phys. Rev. B **86**, 214514 (2012).
- ³² H. Wei, S.-P. Chao, and V. Aji, ArXiv e-prints (2013), arXiv:1305.7233 [cond-mat.supr-con].
- ³³ The FS index is also a momentum index because it labels Weyl nodes which are generally separated in momentum space.
- ³⁴ S.-Y. Xu, C. Liu, S. Kushwaha, T.-R. Chang, J. Krizan, R. Sankar, C. Polley, J. Adell, T. Balasubramanian, K. Miyamoto, *et al.*, arXiv preprint arXiv:1312.7624 (2013).
- ³⁵ Z. K. Liu, B. Zhou, Y. Zhang, Z. J. Wang, H. M. Weng, D. Prabhakaran, S.-K. Mo, Z. X. Shen, Z. Fang, X. Dai, Z. Hussain, and Y. L. Chen, Science **343**, 864 (2014).
- ³⁶ S. M. Young, S. Zaheer, J. C. Y. Teo, C. L. Kane, E. J. Mele, and A. M. Rappe, Phys. Rev. Lett. **108**, 140405 (2012).
- ³⁷ Z. Wang, H. Weng, Q. Wu, X. Dai, and Z. Fang, Physical Review B **88**, 125427 (2013).
- ³⁸ L. He, X. Hong, J. Dong, J. Pan, Z. Zhang, J. Zhang, and S. Li, arXiv preprint arXiv:1404.2557 (2014).
- ³⁹ S. Jeon, B. B. Zhou, A. Gyenis, B. E. Feldman, I. Kimchi, A. C. Potter, Q. D. Gibson, R. J. Cava, A. Vishwanath, and A. Yazdani, arXiv preprint arXiv:1403.3446 (2014).
- ⁴⁰ T. Liang, Q. Gibson, M. N. Ali, M. Liu, R. Cava, and N. Ong, arXiv preprint arXiv:1404.7794 (2014).
- ⁴¹ M. Neupane, S.-Y. Xu, R. Sankar, N. Alidoust, G. Bian, C. Liu, I. Belopolski, T.-R. Chang, H.-T. Jeng, H. Lin, *et al.*, Nature Communications **5** (2014).